Journal of Nuclear Materials 393 (2009) 311–320

Contents lists available at ScienceDirect

Journal of Nuclear Materials

journal homepage: www.elsevier.com/locate/jnucmat

Microstructural development in irradiated U-7Mo/6061 Al alloy matrix dispersion fuel

Dennis D. Keiser Jr. [a,*], Adam B. Robinson [a], Jan-Fong Jue [a], Pavel Medvedev [a], Daniel M. Wachs [a], M. Ross Finlay [b]

[a] Nuclear Fuels and Materials Division, Idaho National Laboratory, P.O. Box 1625, Idaho Falls, ID 83415-6188, USA
[b] Australian Nuclear Science and Technology Organization, PMB 1, Menai, NSW 2234, Australia

ARTICLE INFO

Article history:
Received 26 February 2009
Accepted 15 June 2009

ABSTRACT

A U-7Mo alloy/6061 Al alloy matrix mini-dispersion fuel plate was irradiated in the Advanced Test Reactor and then examined using optical metallography and scanning electron microscopy to characterize the developed microstructure. Results were compared to the microstructure of the as-fabricated dispersion fuel to identify changes that occurred during irradiation. The layer that formed on the surface of the fuel U-7Mo particles during fuel plate fabrication exhibits stable irradiation performance as a result of the ~0.88 wt% Si present in the fuel meat matrix. During irradiation, the pre-formed interaction layer changed very little in thickness and composition. The overall irradiation performance of the fuel plate to moderate power and burnup was considered excellent.

1. Introduction

The Reduced Enrichment for Research and Test Reactors (RERTR) program is developing low-enriched uranium (LEU) U-Mo fuels to replace highly-enriched uranium (HEU) fuels in research and test reactors [1]. As part of this development, a variety of irradiation experiments have been conducted in the Advanced Test Reactor (ATR), with the recent focus being on the performance of U-Mo alloy fuels [2]. Initial irradiation testing of U-Mo dispersion fuels with pure Al as the matrix indicated that porosity can develop at high burnups, which may result in pillowing and eventual failure of fuel plates [3]. The porosity initiates and grows within the reaction product, which results from interdiffusion between the U-Mo fuel and the Al matrix. Si additions to the matrix of a dispersion fuel may constitute a possible solution to this pillowing problem, since it may result in the stabilization of a U-Al_3-type of phase that exhibits better irradiation performance [4]. Diffusion studies and characterization of as-fabricated U-Mo dispersion fuels have shown that the presence of Si in an Al alloy does result in a change in the types of phases that will form when U-Mo fuels interact with the Al alloy matrix [5–7]. With respect to the irradiation performance of interaction phases that contain Si, it has been demonstrated that U_3Si_2 dispersion fuels, which form a $U(Al,Si)_3$ interaction phase around the fuel particles due to interactions with the Al matrix, perform well under irradiation [8].

To test the effects on irradiation behavior of adding Si to the matrix of U-Mo dispersion fuels, a Si-containing fuel plate, designated R1R010, was irradiated as part of the RERTR-6 experiment using the ATR [9,10]. The Si-containing fuel plate employed 6061 Al alloy as the matrix. The 6061 Al alloy contains around 0.88 wt% Si. The RERTR-6 experiment tested the fuel plate to moderate burnup, flux, and temperatures [10]. During post-irradiation examination (PIE) of the fuel plate, destructive examinations were performed using optical metallography (OM) and scanning electron microscopy (SEM). For the SEM analysis, a scanning electron microscope was used to capture backscattered and secondary electron images of the microstructures of two samples taken from the irradiated fuel plate. Attached wavelength-dispersive and energy-dispersive spectrometers (WDS/EDS) were employed to determine the amounts of various elements in the fuel, interaction zone, and matrix using X-ray mapping, linescans, and point-to-point analysis. This paper describes the results of the examinations that were performed on the U-7Mo fuel with the 6061 Al alloy after irradiation. Particular focus is given to the partitioning behaviors of U, Mo, Al, and Si; the distribution of a variety of fission products; and the distribution of fission gas bubbles that were observed in the U-7Mo fuel particles. Comparisons are made to the original, as-fabricated state of the U-Mo dispersion fuel and to some experimental results that have been reported for irradiated U-Mo dispersion fuels with Al or Al-2Si alloy as the matrix.

2. Fuel plate fabrication

The dispersion fuel fabricated for the RERTR-6 irradiation experiment used powder produced by the Korean Atomic Energy Institute using a rotating-disk centrifugal atomization process [11]. The powder size distribution is enumerated in Table 1, and

* Corresponding author. Tel.: +1 (208) 533 7298; fax: +1 (208) 533 7863.
E-mail address: Dennis.Keiser@inl.gov (D.D. Keiser Jr.).

0022-3115/$ - see front matter © 2009 Published by Elsevier B.V.
doi:10.1016/j.jnucmat.2009.06.018

Table 1
The size ranges of the U-7Mo powders used to fabricate the dispersion fuel plates for the RERTR-6 experiment. The results are normalized by percentage.

Size range (μm)	Percentage of powders in each size range for RERTR-6 plates (%)
>150	0.01
106–150	3.40
75–106	22.34
63–75	20.41
45–63	24.91
38–45	9.21
<38	19.71
Total fines (<45 μm)	28.93

it can be seen that the majority of the particles were less than 106 μm.

The dispersion fuel plates for the RERTR-6 irradiation experiment were fabricated at Argonne National Laboratory using a roll-bonding process that had been used to fabricate earlier RERTR experimental fuels [12]. To make dispersion fuel meat for the R1R010 fuel plate, the U-7Mo powder was blended with 6061 Al alloy powder to have a target fuel loading of 6 g U/cm^3. The 6061 Al alloy powder has a composition, measured by chemical analysis, of 0.99 Mg–0.88Si–0.27Cu–0.17Cr–0.07Fe–balAl. The blended powder was then formed under pressure into a compact. The compacts were placed in the cavity of a 6061 Al alloy "picture frame" and cover plates were added to form the top and bottom cladding. This assembly was welded together and rolled to form a plate of proper thickness. Specifically, the plates were hot rolled in five passes, where the plates were in the furnace approximately 100 min at 500 °C and 15 min outside the furnace during the actual rolling, for a reduction of approximately 85%. The plates were then cold rolled a further 10–15% (in two or three passes) to achieve the final thickness, rough sheared, and shipped to INL for final processing. The nominal fuel zone was rectangular, having a length of 8.1 cm, a width of 1.9 cm, and a uniform thickness of 600 μm. The 6061 Al cladding thickness for dispersion fuels is nominally 400 μm. Therefore, the nominal fuel zone volume was 0.957 cm^3. Uranium enrichment was specified to be 19.7% in the RERTR-6 fuel plates. The final high-temperature process the RERTR-6 fuel plates were exposed to was a blister annealing step where the fuel plates were exposed to approximately 485 °C for approximately 60 min to ensure that no blisters developed on the surface, which would be an indication of poor bonding between the fuel meat and the cladding.

The typical microstructure of a dispersion fuel plate with a Si-containing Al alloy matrix just before it is inserted into the ATR is presented in Fig. 1. Si X-ray mapping shows how Si-rich interaction layers have developed around the U-7Mo fuel particles during fabrication and subsequent blister annealing. Point-to-point composition analysis shows that other matrix alloying constituents (e.g., Mg, Cu, and Cr) are present in the interaction layers.

3. Irradiation testing

The RERTR-6 experiment tested fuel materials to average burnups (BU) of 35–49% depending on experiment location with a peak heat flux of <220 W/cm^2 and a beginning-of-life temperature of <200 °C. The experiment was irradiated in the ATR West B12 irradiation test position during cycles 134B, 135B, and 135C, and it remained in the reactor for 135.1 effective full power days (EFPD). The RERTR-6 irradiation test assembly held four capsules, axially designated as A through D from the top of the test assembly to the bottom. Each capsule had two levels, with four mini-plate positions per level, giving eight mini-plate positions per capsule. There were 32 mini-plate positions per test assembly. Due to the orientation of the fuel plates, where one edge of a fuel plate faced the core, there was a large neutron flux gradient across the width of the plates. For the mini-plate comprised of U-7Mo particles dispersed in 6061 Al alloy matrix (labeled R1R010), the average BU was 40.8% (57.1% at the edge facing the core and 30.6% on the other side). Two samples were generated for SEM analysis, one from the low-burnup side (R1R010A) and one from the high-burnup side (R1R010B). Fig. 2 shows the fission rate history for the two samples.

Calculations were performed using the fuel performance computer code, PLATE [13], to determine some local performance metrics at fuel plate locations where the SEM samples were generated. Recently, the swelling and interaction layer growth models in the PLATE code have been updated [14,15]. The calculated parameters included heat flux and peak temperature (see Figs. 3 and 4). The calculations were based on the nominal dispersion fuel plate design, the fuel plate as-built data, and the power history calculated by Chang et al. [16].

4. Post-irradiation examination

4.1. Optical metallography

After irradiation of the fuel plate, microstructural analysis was performed using OM. A complete transverse cross-section of the

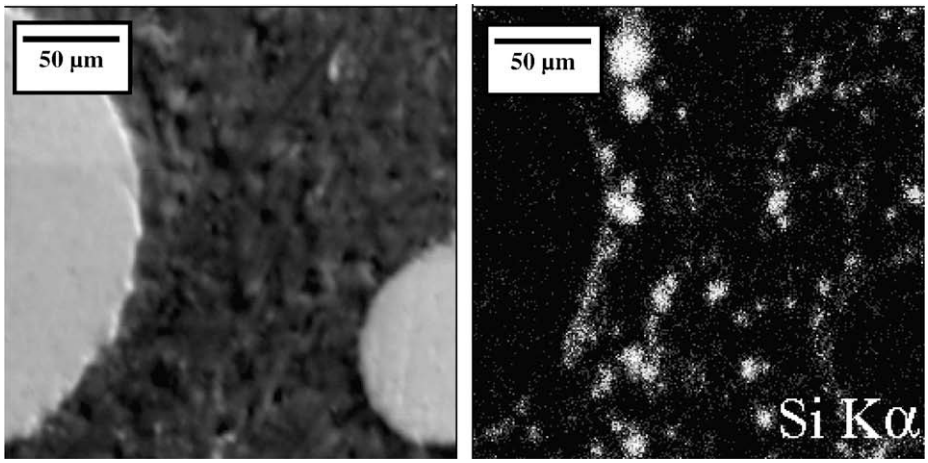

Fig. 1. SEM micrograph (left) of U-7Mo particles (bright) and matrix (dark) in a typical as-fabricated dispersion fuel that has a Si-containing Al alloy matrix. The Si WDS X-ray map (right) shows the Si-rich precipitates in the matrix and the Si-rich interaction layers that are present around the U-7Mo particles.

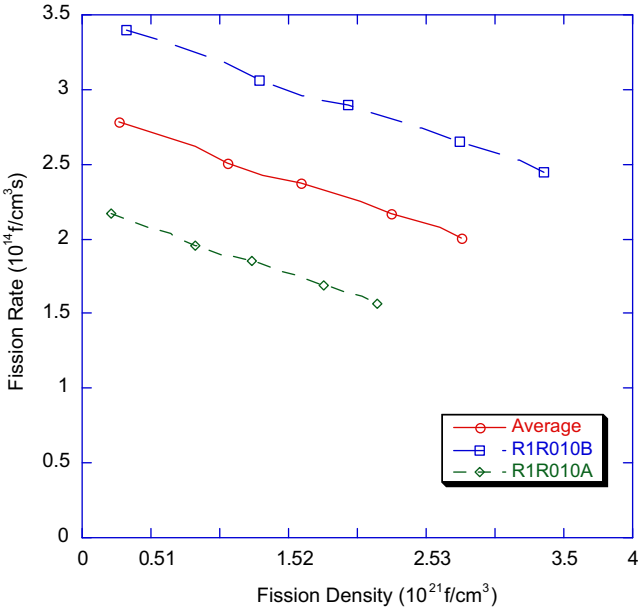

Fig. 2. Fission rate history for the fuel contained in samples R1R010A (outer edge) and R1R010B (core edge). A comparison of the R1R010A and R1R010B histories shows the large neutron flux gradient that was present across the width of the R1R010 fuel plate. Burnup is at% of ^{235}U fissioned.

plate, taken at the midplane, was mounted in epoxy, polished using 1200-grit sandpaper, and examined in the etched and un-etched conditions. Fig. 5 shows the microstructure of a complete cross-section of RERTR-6 fuel plate R1R010 and some images at higher magnification. The side of the plate that faced the core, which was exposed to the highest neutron flux, is labeled "hot," and the edge exposed to the lowest flux is labeled "cold". Overall, the microstructure consists of U-7Mo fuel particles homogeneously distributed in the 6061 Al matrix, with narrow fuel/matrix interaction layers present around the fuel particles.

4.2. Scanning electron microscopy

Two 1-mm-diameter, cylindrical punchings were taken through the nominally 1.9-cm-wide, 0.06-cm-thick fuel meat of fuel plate R1R010 at the INL Hot Fuel Examination Facility (HFEF) for SEM

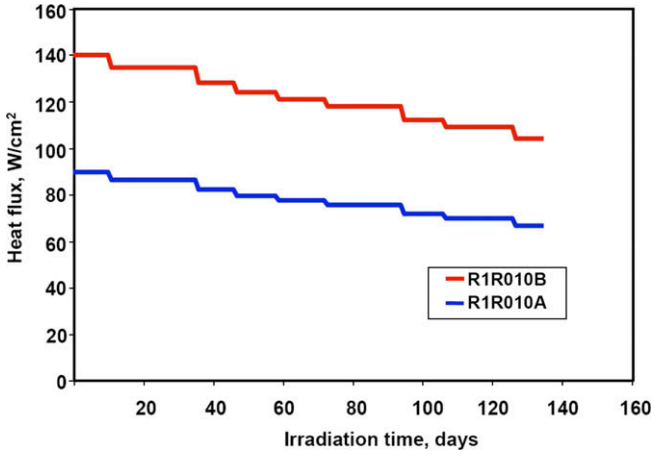

Fig. 3. Evolution of the heat flux within punching R1R010B (top plot) and R1R010A (bottom plot). The heat flux history follows the local power history. The "step" decreases in the heat flux are due to the neutronic analysis assumption of the constant power over a specified time.

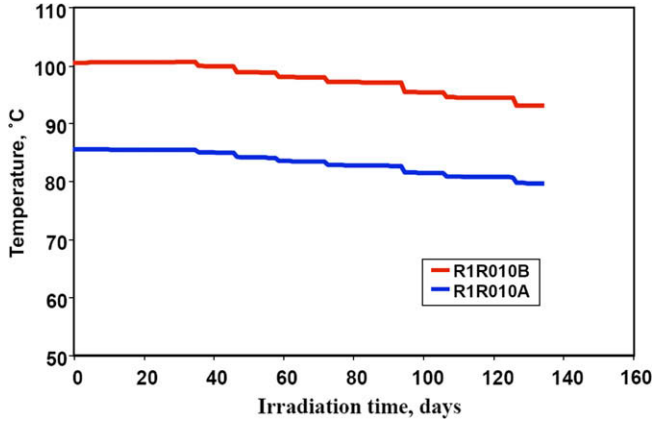

Fig. 4. Peak temperature within punching R1R010B (top plot) and R1R010A (bottom plot).

analysis. This was accomplished by using a commercially available press that had been modified for easier operation in a hot cell environment [17]. Samples R1R010A (low flux side) and R1R010B (high flux side) were transferred to the Electron Microscopy Laboratory (EML) for sample preparation and analysis. Since this analysis took place more than three years after the fuel plates had been discharged from ATR, handling of these relatively small samples was manageable in an air glovebox. The punchings were mounted longitudinally in a phenolic ring using an epoxy mixed with 325-mesh tungsten powder to provide shielding. The samples were then polished with progressively finer grit sandpapers, finishing with 1200-grit. The mounted samples were coated with Pd and inserted either into a ZEISS Model 960A SEM that was equipped with an Oxford WDS and EDS that employed ISIS LINK software or a JEOL JSM-7000F field emission gun SEM with WDS and EDS and Oxford INCA software. Backscattered electron and secondary electron images were generated to examine the fuel microstructure, and the spectrometers were employed to generate X-ray maps and linescans and perform semi-quantitative point-to-point compositional analysis to determine the presence of various elements in the fuel, interaction zone, and matrix. The Oxford INCA computer software corrected for the 50 nm-thick layer of Pd coating on the sample when it determined phase compositions.

The microstructures observed in the optical micrographs taken of fuel plate R1R010 indicated that the punching microstructures are comprised of U-7Mo particles with approximately 1–2 μm-thick interaction layers around the fuel particles. Fig. 6 shows a SEM image of the microstructure that was observed for samples R1R010A and R1R010B. Higher magnification images for R1R010A (Fig. 7) and R1R010B (Fig. 8) show that narrow interaction layers were present around the fuel particles. X-ray mapping was employed using WDS to identify the partitioning behavior of the U, Mo, Al, and Si. Fig. 9 shows the partitioning behavior observed for sample R1R010A. U, Mo, Al, and Si were observed in the interaction layers. Si was also found in precipitates in the 6061 Al alloy matrix. Some areas of the matrix, immediately adjacent to the fuel particles, were devoid of Si precipitates. This was probably because during irradiation, recoil-zones are created around the fuel particles [18], which extend about 10 μm into Al. The fission fragment tracks cause the original Si-rich precipitates to dissolve, leaving behind precipitate-free zones (PFZ). Point-to-point composition analysis, which is typically performed to determine the composition of the Si-rich interaction layers, could not be performed in many areas of the fuel plate due to the narrow thickness of the layer. However, one area was found in R1R010B where a reasonable amount of interaction layer was observed (see Fig. 8a),

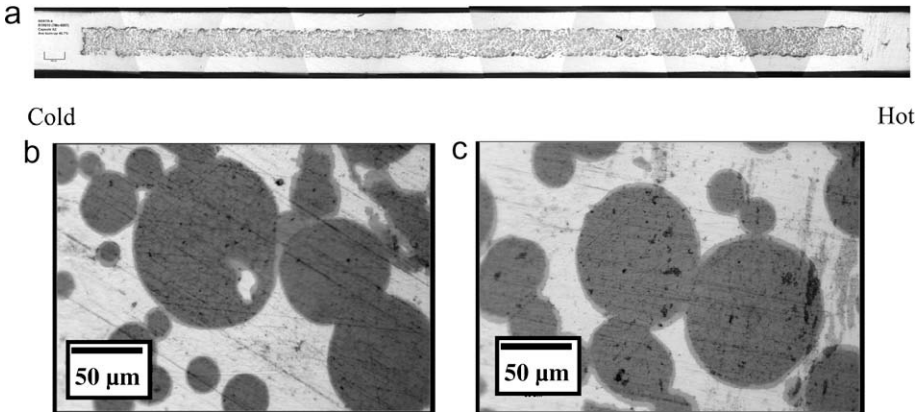

Fig. 5. Optical micrographs of (a) the microstructure of a transverse cross section taken at the mid-plane of fuel plate R1R010, (b) the microstructure in an area near the "cold" edge of the plate, and (c) the microstructure near the "hot" edge of the plate.

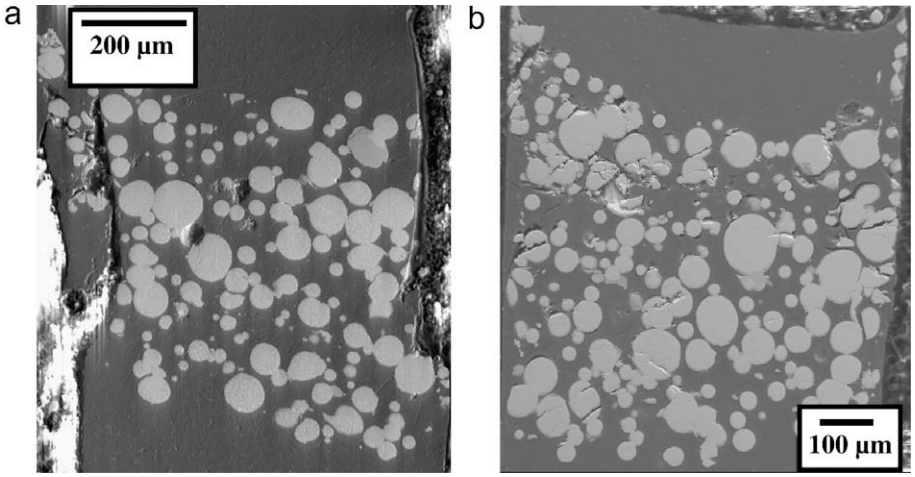

Fig. 6. Secondary electron images of the longitudinal cross sections of the two punchings (a) R1R010A and (b) R1R010B. The bright contrast phases are U-7Mo particles contained in the darker 6061 Al matrix.

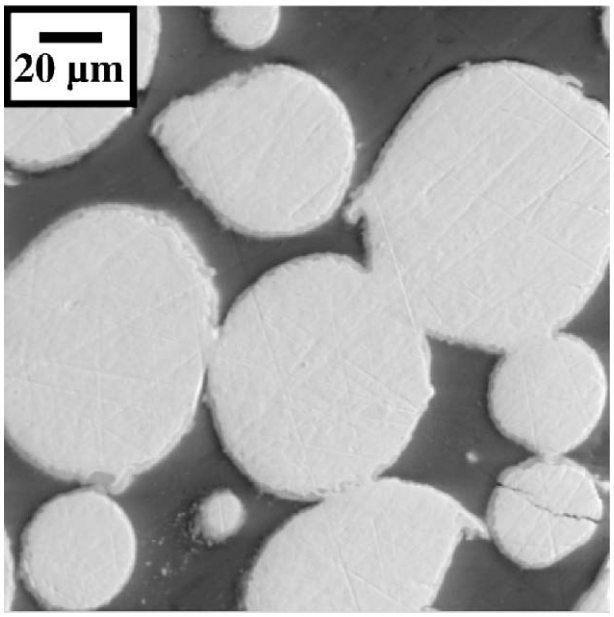

Fig. 7. Secondary electron image of the microstructure for sample R1R010A where relatively thin interaction layers (medium gray) were observed around the U-7Mo (bright contrast) particles.

and the interaction layer composition at this location was found to be approximately 24U-64Al-11.Si–0.3 Mg, in at% (see Table 2) with negligible Mo. Due to overlap issues with the Kα X-ray peaks for Mg, Al, and Si, this composition is just qualitative. Since both the cladding and the fuel meat matrix of this fuel plate were 6061 Al, Si X-ray maps were generated at different locations along the cladding/fuel meat interface to compare the amount of Si-rich precipitate phases present in the cladding vis-à-vis the matrix. Fig. 10 shows a Si X-ray map that was produced at the fuel meat/cladding interface in the R1R010B sample. There are clearly more precipitates above the interface into the cladding. Most of the Si-rich precipitates have been consumed in the fuel meat matrix due to thermal diffusion during fuel fabrication or due to radiation enhanced diffusion during irradiation, which resulted in the creation of Si-rich interaction layers around the U-7Mo particles.

With respect to the fission product Xe, X-ray mapping showed that this element was uniformly distributed in the fuel particles, and extended into the 6061 Al matrix. Fig. 11 shows X-ray maps for Xe, U, Mo, Al, Si, and Mg. Nd, Cs, Ru, and Zr were also mapped and observed to be uniformly distributed through the U-7Mo particles. To determine how fission gas bubbles are distributed in the microstructure of the U-7Mo particles, high magnification images were generated from fracture surfaces. Fig. 12 shows the fission gas bubble distribution in a fractured U-7Mo particle observed in the R1R010B sample. It can be seen that the U-7Mo alloy irradiated

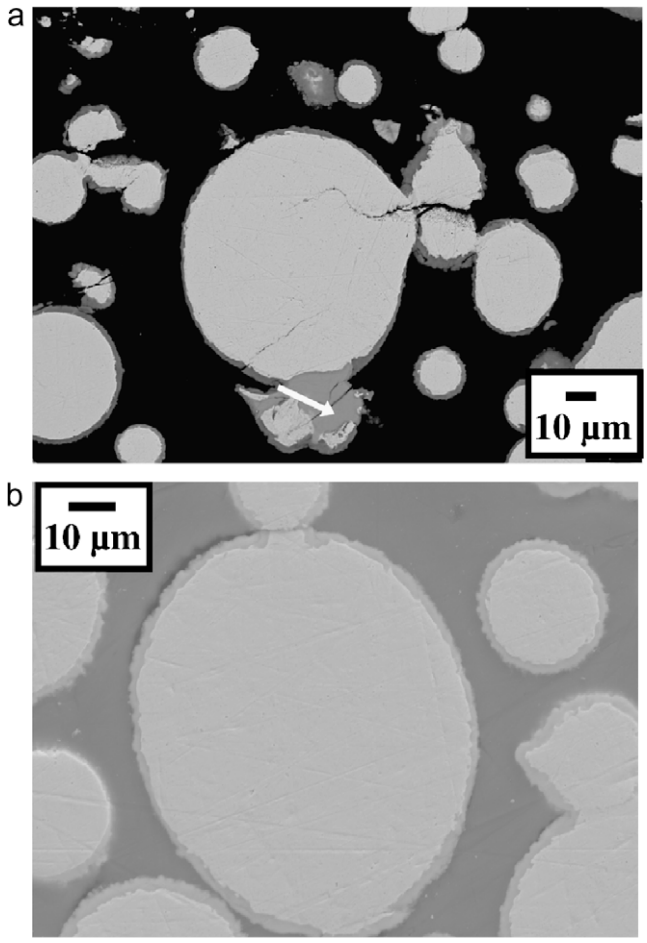

Fig. 8. Backscattered (a) and secondary electron (b) images of sample R1R010B showing the relatively thin interaction layers (medium gray) around the U-7Mo (bright contrast) particles. In (a) an area with a relatively large amount of interaction layer present (arrow) is shown.

to <50% U-235 burnup has many fission gas bubbles on the grain boundaries, and in only a few cases interior to the grains. This overall fission gas behavior contributed to the 17.3% estimated fuel swelling and 3.9% average plate swelling of the R1R010 fuel plate that was measured during PIE.

5. Discussion

5.1. Comparison to the literature

To develop better understanding of how adding Si may be affecting the microstructural development of the fuel meat during irradiation, it is beneficial to make comparisons with irradiation performance data that is available in the literature. Table 3 lists relevant data from reactor experiments that have been conducted using U-Mo dispersion fuels including interaction-layer development. The IRIS-1 experiment tested a dispersion fuel of U-7.6 wt% Mo and Al in the OSIRIS reactor [19,20]. The U-Mo fuel was in the form of ground powder. To perform SEM and electron probe micro-analyzer (EPMA) analysis of the IRIS-1 fuel, three 15.4-mm-diameter punching samples were used. All of the samples displayed identical microstructures, where only small amounts of residual Al were present in the fuel meat, fine fission gas bubbles could be observed in the U-Mo grains, and large areas of a reaction product, which were free of fission gas bubbles, decorated the U-Mo particles. Contrary to IRIS-1, the IRIS-2 [21] and FUTURE [3,22] experiments used atomized U-Mo powders dispersed in Al, and these plates also contained fission gas bubbles in the U-Mo particles, interaction layers around the particles, and no fission gas bubbles in the interaction layers. Both the IRIS-2 and FUTURE fuel plates experienced excessive pillowing. It was observed that large pores developed at the interface between the interaction layer and the unreacted Al. Listed in Table 3 are details about the interaction layer composition for the various irradiation tests. For the FUTURE experiment, a phase with a composition of 15U–3Mo–82Al (at%) was observed. For IRIS-2, changes in interaction product composition were observed as a function of moving from the "pillowing area" area of the plate (Al/(U + Mo) ratio of 4.5) to the edge of the meat (Al/(U + Mo) ratio of 6). The ratio of 6 was at the coldest plate region and 4.5 at the hottest. For the lower temperature IRIS-1 test, a ratio of up to 8 was reported, and for the FUTURE test, which was at a higher temperature, the ratio was reportedly 3–4. The IRIS-3 experiment tested a U-7.3 wt% Mo dispersion fuel with Al-2.1 wt% Si alloy as the matrix, instead of the pure Al that was employed in IRIS-1 and FUTURE [23,24]. The PIE showed an uneven U-Mo-Al interaction layer had formed around the U-Mo particles, and X-ray maps showed that layers enriched in Si were present at some locations. Overall, the thinnest layers corresponded to areas with the highest concentrations of Si, and it was suggested that Si precipitates were present near the thinnest layers. The most commonly observed phase had an (Al + Si)/(U + Mo) ratio near 4, and this phase was not highly enriched in Si. Around 2.0 wt% (~5 at%) Si was the highest concentration reported. For IRIS-TUM, an Al/(U + Mo) ratio of 3 to 4 was reported for the interaction layers [25]. For the R1R010B sample characterized in this study, an approximate (Al + Si)/(U + Mo) ratio of 3 was observed.

The data discussed above is for plate-type fuels, but observations from irradiated pin-type fuels that were run as part of the KOMO-2 [26] and KOMO-3 [27] experiments can also be compared. For KOMO-2, in the fuel regions of the pin-type fuels that consisted of U-7Mo atomized particles in Al that reached 50%, 62%, and 68% burn-ups, compositional analysis was performed on the interaction layers. In general, there was very little change in composition throughout the thickness of the interaction layers; for the lower temperature regions of the fuel, a $(U,Mo)Al_4$ phase was observed, and in the higher temperature regions, a $(U,Mo)Al_3$ phase was observed, which is not observed in plate-type fuels. The $(U,Mo)Al_4$ phase had an approximate composition of 15U–3Mo–82Al. The beginning-of-life (BOL) temperatures that were calculated for the 50%, 62%, and 68% burnup samples were 134.2 °C, 167.3 °C, and 188.9 °C, respectively. The peak fuel temperatures for these samples were calculated to be 143 °C, 280 °C, and 334 °C, respectively. All three of the samples that saw different burnups formed a $(U,Mo)Al_4$ phase in the center and/or outer periphery of the fuel.

For the KOMO-3 experiment, the performance of fuel plates with atomized U-7Mo fuel particles and Al or Al-2.0 wt% Si alloy matrices were compared. The fuel pin with Al matrix was irradiated to 63.2% burnup at the fuel meat center and had a maximum BOL temperature of 170 °C, while the Al-2.0 wt% Si matrix fuel element was irradiated to 64.87% burnup at the fuel meat center and had a maximum BOL temperature of 174 °C. It was observed that the composition of the interaction layers that formed at the interface between the U-7Mo fuel particles and the matrix were very similar regardless of whether the matrix was Al or Al-2.0 wt% Si. A $(U,Mo)Al_3$-type phase was observed for the highest temperature regions of the fuel elements, and a $(U,Mo)Al_4$-type phase was observed to develop in the colder regions. For the fuel element with Al-2.0 wt% Si matrix, up to 11.0 at% Si was measured in the $(U,Mo)(Al,Si)_3$ phase and up to 4.0 at% Si was observed in the $(U,Mo)(Al,Si)_4$-type phase. Overall, the interaction layer thickness was decreased for the fuel with a Si-containing matrix (~40 μm) compared to the one that had pure Al (~70 μm).

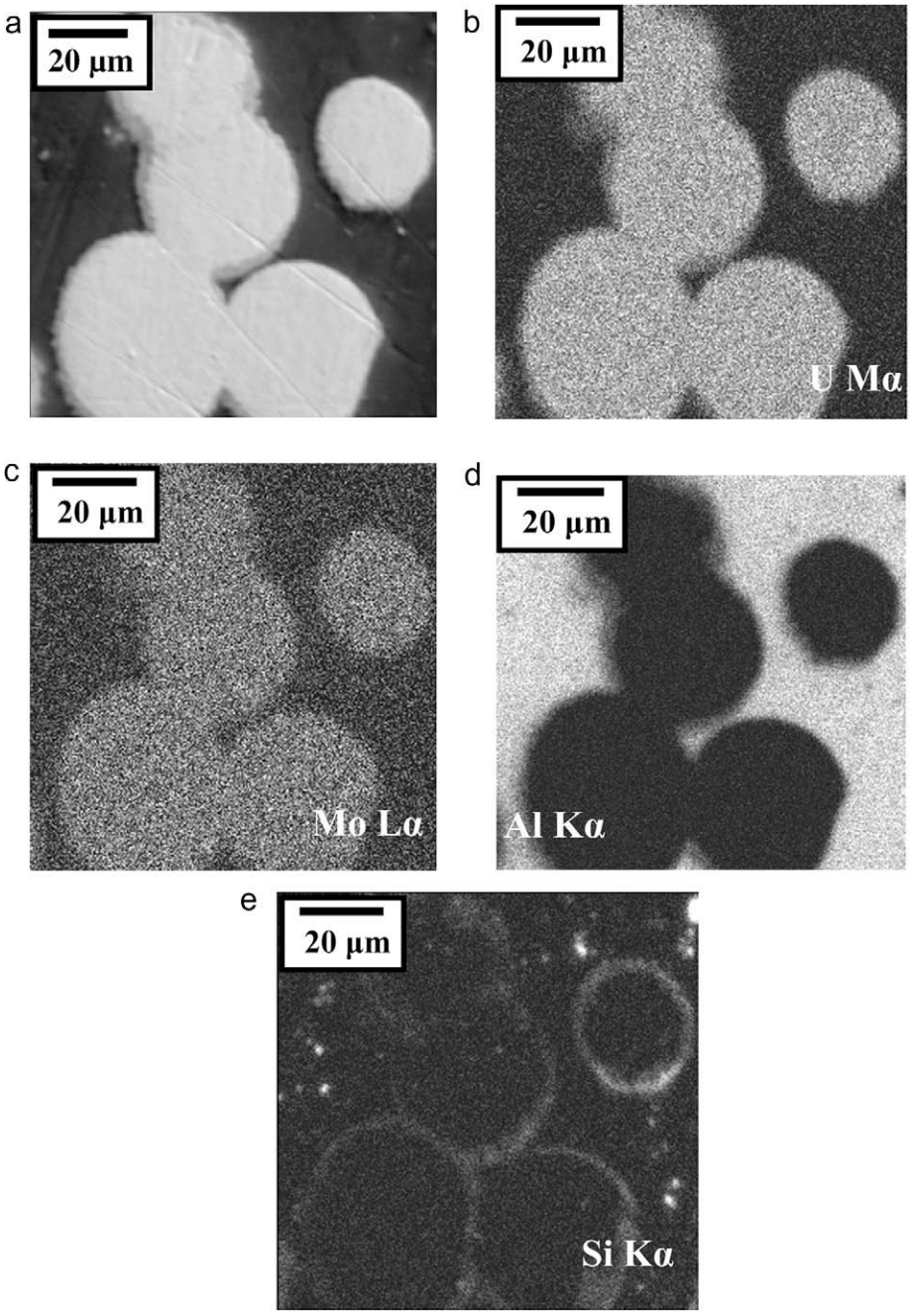

Fig. 9. Secondary electron image (a) and WDS X-ray maps for (b) U, (c), Mo, (d) Al, and (e) Si for the R1R010A sample.

Table 2
EDS composition of interaction layer, in at%, at the location indicated in Fig. 8a.

Point	Mg	Al	Si	U	Mo
1	0.5	60.6	14.2	24.7	Negligible
2	0.3	64.9	9.9	24.7	Negligible
3	0.2	66.2	9.0	24.6	Negligible
4	0.3	64.4	12.7	22.5	Negligible

5.2. Development and behavior of Si-rich layers

Based on the results from the literature, there is general agreement with the idea that adding Si to the matrix improves U-Mo dispersion fuel plate performance. In general, the amount of interaction is reduced and more stable fuel behavior is observed. In other words, the gross porosity that can link up and cause fuel failure is not observed. This agrees with the observations made as part of the current investigation. One difference between the samples looked at in this paper and those used in the experiments described in Table 3 is the fact that pre-existing Si-rich layers were present around the fuel particles for the R1R010 fuel plate, which were probably not present in the as-fabricated, Si-containing matrix fuel plates irradiated in the IRIS-3 and IRIS-TUM experiments. The rolling temperatures used to fabricate the IRIS-3 and IRIS-TUM fuel plates are typically lower than those used to fabricate the fuel plates discussed in this paper, but any blister annealing process for the IRIS plates would have been similar to what was employed for R1R010. During the rolling process, the softer AlFeNi (IRIS-TUM) and AG3NE (IRIS-3) claddings can be rolled at lower temperatures

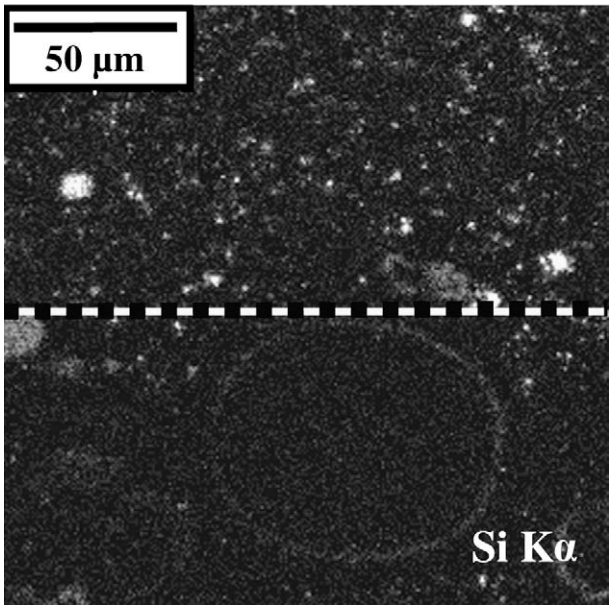

Fig. 10. Si WDS X-ray map at a location along the cladding/fuel meat interface (dashed line).

(in the mid-400 °C range compared to 500 °C). Rolling at temperatures lower than 500 °C has a significant impact on the amount of interaction that will occur between U-7Mo and Al alloys. First, it reduces the overall kinetics of the interaction, since diffusion rates are lower at lower temperatures. Second, and perhaps more significantly, decomposition of the γ-phase U-7Mo alloy has been found to start within times as short as 10 min at 500 °C [28], and this decomposition significantly increases the rate of interaction for a U-7Mo alloy with 6061 Al alloy compared to pure γ-phase alloys [5]. The nose of the Time Temperature Transformation (TTT) curve for γ-phase U-Mo alloys to begin transforming to $\alpha - U + \gamma'$ (U_2Mo) is near 500 °C [29,30]. Therefore, temperatures in the mid-400 °C range are below the nose of the TTT curve, and as a result it takes hours before γ-phase U-7Mo starts to decompose and increase interaction rates. So, if during fabrication the U-7Mo alloy remains γ-phase, the interaction rates with Al alloys are much more sluggish [5]. Even in cases where U-7Mo particles decompose during fabrication, they will revert to γ-phase when they are irradiated [31].

When dispersion fuels do not form a layer during fabrication, any interaction layer that is present after irradiation is formed due to radiation-enhanced diffusion (RED). The temperatures that fuel plates are exposed to during irradiation are low enough (typically around 100 °C and at most 200 °C) such that any thermal diffusion component should be negligible. Therefore, any interaction that takes place appears to be due to RED. Si present in interaction layers created by RED probably should come from the Si that is present as precipitates in the matrix alloy in the recoil zones around the fuel particles (~10 μm). The fission fragments and localized heating from thermal spikes in these regions result in Si diffusion to the U-7Mo/matrix interface where it participates in phase formation. Alternatively, for the fuels where Si-rich phases are created during fabrication, Si diffuses to the interface due to thermal diffusion at the near-500 °C fabrication temperatures and is present in the phases in the formed layers. Some of the Si can come from locations in the matrix that are farther away than the thickness of a recoil zone. As a result, a Si-rich layer is already present when the irradiation process takes place. Diffusion studies using U-7Mo and 6061 Al performed at 500 °C have shown that Si-rich interaction layers can form that have Si concentrations that vary between 13 and 48 at% Si [5]. In diffusion studies conducted with U-7Mo and 6061 Al performed at 550 °C, interaction layers with 11 at% Si were observed, and XRD results suggested that a $U(Al,Si)_3$ phase was present at the U-7Mo/6061 Al interface [32]. Based on the approximate layer composition of 24U-64Al-11Si–0.3 Mg, in at%, that was measured for the irradiated R1R010B sample, it appears that the interaction phase that is present after the irradiation process has a Si concentration that is similar to what is expected for phases that form during fabrication.

A full understanding of the performance of as-irradiated U-Mo dispersion fuels with matrices that contain Si seems to require that more samples be characterized using a SEM or electron microprobe to develop better understanding of how making additions to the matrix or fuel will affect the formation of interaction layers. Samples with varying Si additions to the matrix that have been irradiated under a variety of conditions should be analyzed in an attempt to determine the mechanisms by which the presence of Si in the matrix influences interactions with the fuel. This work should also include the use of X-ray diffraction so that the crystal structures of the developed phases can be determined. It has been shown that in U-Mo dispersion fuels with Al as the matrix that have been irradiated at relatively low temperatures, the interaction layers that form are amorphous [33], and amorphous layers may display different performance characteristics relative to phases that are crystalline. As a result, it is of interest to determine if interaction layers that form in U-Mo dispersion fuels with Al alloys that contain Si as the matrix are also amorphous. Finally, the impact of other alloy components, like the Mg that is observed in the developed interaction layers for R1R010A and R1R010B, needs to be considered.

With respect to determining how fission products partition between fuel phases in irradiated dispersion fuels with matrices that contain Si, it seems that Nd, Xe, Cs, Zr, and Ru all distribute uniformly through the U-7Mo particles. In [8] uniform distributions for Xe and Nd were observed within the U-7Mo particles in an irradiated Al matrix dispersion fuel, and at the interaction layer/matrix boundary the Xe was observed to be locally enriched, possibly because the Xe was transported with the growing interaction layer during irradiation. For sample R1R010A and R1R010B, the Xe did not seem to localize, but instead it extended a distance into the 6061 Al matrix, possibly due to fission fragment recoil.

Fission gas bubble swelling has been described in [34]. Based on the characterization of many irradiated dispersion fuels, it has been found that the fission gas bubbles first appear on the grain boundaries at low burnups, with virtually no bubbles interior to the grains. For fuels that employ atomized U-Mo fuel particles with a cored microstructure, this microstructure is reported to disappear by 39% ^{235}U burnup, and the fission gas bubbles concentrate on primary grain boundaries [35]. At around 40–50% ^{235}U burnup, the bubble population on the grain boundaries increases, and larger bubbles start to form internal to the grains. At this point, recrystallization starts to take place and the fuel begins to swell at a faster rate. At the higher burnups, the gas bubbles will uniformly distribute throughout the fuel microstructure. The microstructure that was observed for the RERTR-6 fuel plate R1R010, irradiated to around 50% ^{235}U burnup, agrees with the description above. At this level of burnup, one would expect to observe many fission gas bubbles residing on grain boundaries, along with areas where the fission gas bubbles have grown larger internal to the grains. This is exactly what has been observed for the RERTR-6 sample R1R010B. For cases where gas bubbles cannot be observed internal to the grains, the bubbles are actually present, but at a very small size. It has been shown that the gas bubbles are approximately 2 nm in size and reside on an ordered superlattice, with a spacing of around 6–7 nm between the bubbles [33].

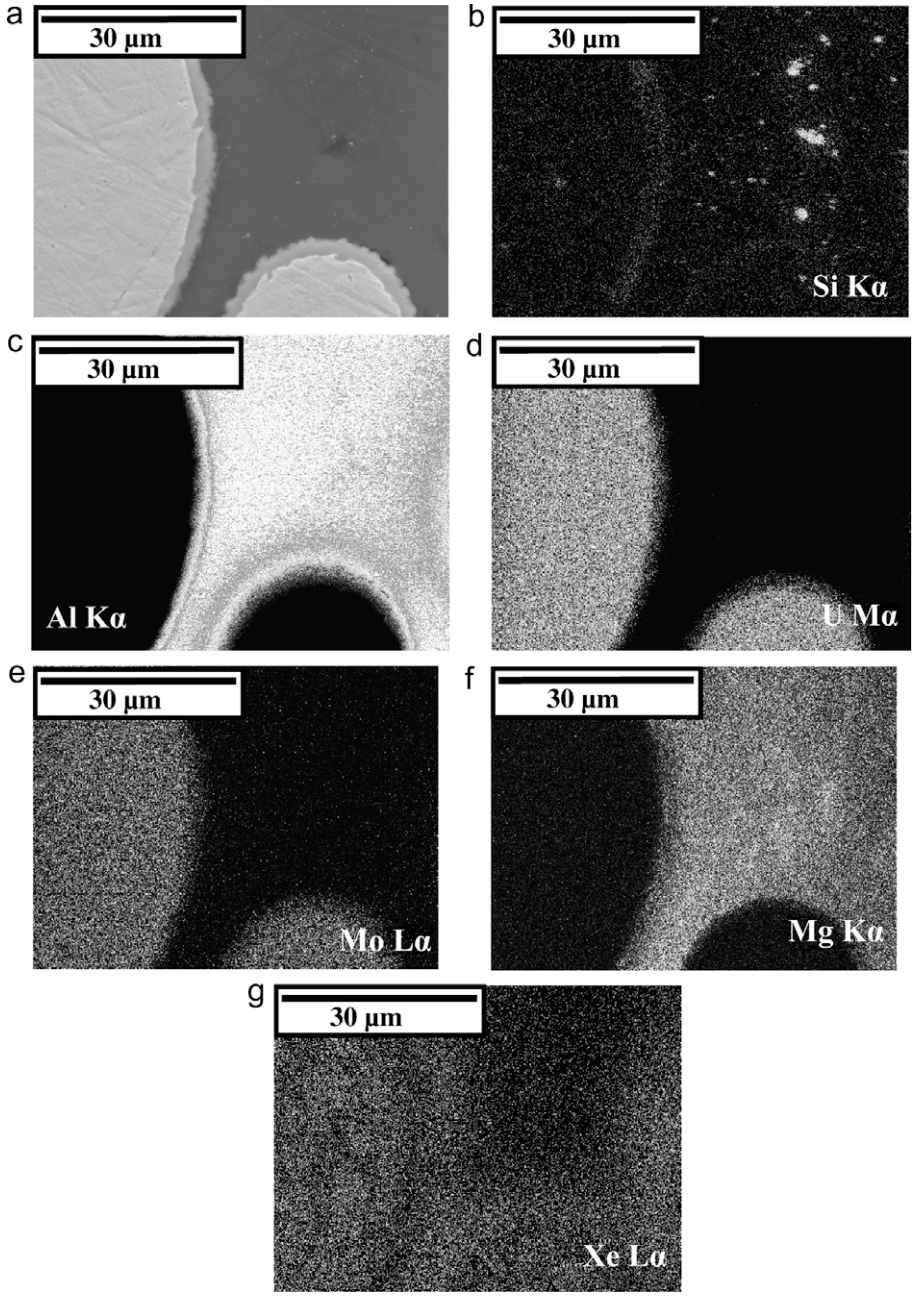

Fig. 11. Secondary electron image (a) and WDS X-ray maps for (b) Si, (c) Al, (d) U, (e) Mo, (f) Mg, and (g) Xe for the R1R010B sample.

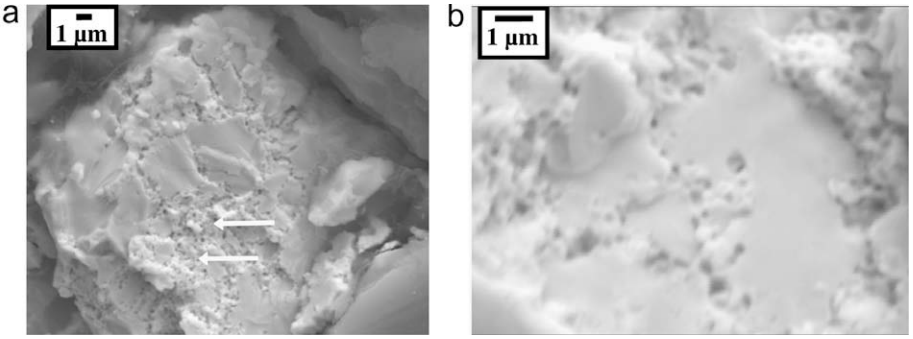

Fig. 12. Secondary electron images of a U-7Mo particle fracture surface observed in the R1R010B sample. Fission gas bubbles can be observed on grain boundaries and internal to some grains (see arrows in (a)).

Table 3
Comparison of the calculated values for peak temperature, fission density, fission rate, peak heat flux, and interaction zone thickness for samples R1R010A and R1R010B with those reported for the irradiated dispersion plates IRIS-1 [20], IRIS-2 [20], IRIS-3 [20,23], IRIS-TUM [20,24,25], and FUTURE [3,22].

Experiment (sample)	Matrix	Calculated peak cladding temperature (°C)	Fission density (plate, sample, average) (10^{21}f cm^{-3})	Average fission rate (burnup) (10^{14}f cm^3 s^{-1})	Peak heat flux for entire plate or punching (W/cm^2)	Interaction zone thickness (μm)	Al/(U + Mo) ratio
IRIS-1	Al	69	3.2	1.5	124	4–6	6[a]–8[b]
IRIS-2	Al	93	2.2	4.4	238	7–10	4.6–5.8
IRIS-3	Al–2Si	83	3.4	3.0	196	1–6	~4[c]
IRIS-TUM	Al	103	4.2	3.6	~250	~5	3–4
IRIS-TUM	Al–2Si	103	4.2	3.6	~250	~5	3–4[c]
FUTURE	Al	130	1.4	6.3	353	4[d]–11[e]	3.3–4.7
R1R010A	6061 Al	87[f]	1.3	1.8	90	~1.5[g]	ND
R1R010B	6061 Al	102[f]	1.9	2.9	140	~1.5[g]	~3[c]

ND: Not Determined.
[a] (For BU = 61%).
[b] (For BU = 67.5%).
[c] Si is combined with Al to get this ratio.
[d] For low heat flux region of plate.
[e] For high heat flux region of plate.
[f] Calculated temperature at punching midplane.
[g] Thickness based on SEM analysis of fuel particles in punching sample.

6. Conclusions

Based on destructive examinations using optical metallography and SEM/EDS/WDS analyses performed on U-Mo dispersion fuel plates with matrices that contained Si that were irradiated in the ATR as a part of the RERTR-6 experiment, the following conclusions can be drawn:

Under the moderate burnup, flux, and temperature conditions of the RERTR-6 reactor experiment, a U-7Mo dispersion fuel with 6061 Al alloy (0.88 wt% Si) matrix exhibits overall thinner interaction layers between the U-7Mo fuel particles and the matrix, compared to U-Mo dispersion fuels with relatively pure Al as the matrix that are irradiated under similar conditions.

For as-fabricated dispersion fuel plates with Al alloy matrices that contain Si that have pre-existing Si-rich interaction layers, there seems to be a difference in fuel behavior during irradiation relative to fuel plates that do not have these layers after fabrication. When fuel plates contain as-fabricated Si-rich interaction layers, these layers do not appear to increase significantly in thickness during irradiation, up to moderate powers and burnup. On the other hand, fuel plates with little or no as-fabricated interaction layers seem to develop micron-thick layers during irradiation that do not appear to be as Si-rich.

Acknowledgments

This work was supported by the US Department of Energy, Office of Nuclear Materials Threat Reduction (NA-212), National Nuclear Security Administration, under DOE-NE Idaho Operations Office Contract DE-AC07-05ID14517. The HFEF staff, located at INL, is thankfully acknowledged for its contributions in performing PIE and generating punchings used for conducting the SEM analysis. Tom Weincek is acknowledged for his efforts in fabricating the dispersion fuels for the RERTR-6 experiment at Argonne National Laboratory. INL staff is also acknowledged for the fabrication of the RERTR-7 experiment. Acknowledgment is given to the ATR staff for their assistance in performing the irradiation experiments.

References

[1] J.L. Snelgrove, G.L. Hofman, M.K. Meyer, C.L. Trybus, T.C. Wiencek, Nucl. Eng. Des. 178 (1997) 119.
[2] D.M. Wachs, D.D. Keiser, Jr., M.K. Meyer, D.E. Burkes, C.R. Clark, G. Moore, J.-F. Jue, M.R. Finlay, T. Totev, G. Hofman, T.C. Wiencek, Y.S. Kim, J.L. Snelgrove, in: Proc. of Global 2007: Advanced Nuclear Fuel Cycles and Systems Conference, Boise, Idaho, 2007.
[3] A. Leenaers, S. Van den Berghe, E. Koonean, C. Jarousse, F. Huet, M. Trotabas, M. Boyard, S. Guillot, L. Sannen, M. Verwerft, J. Nucl. Mater. 335 (2004) 39.
[4] Y.S. Kim, G.L. Hofman, H.J. Ryu, J. Rest, in: Proc. of the 25th International Meeting on Reduced Enrichment for Research Reactors, Boston, MA, 2005.
[5] D.D. Keiser Jr., Defect Diffus. Forum 266 (2007) 131.
[6] E. Perez, N. Hotaling, A. Ewh, D.D. Keiser Jr., Y.H. Sohn, Defect Diffus. Forum 266 (2007) 149.
[7] D.D. Keiser, Jr., J. Gan, J.-F. Jue, B.D. Miller, Mater. Charact. (2009).
[8] A. Leenaers, S. Van den Berghe, E. Koonean, P. Jacquet, C. Jarousse, B. Guigon, A. Ballagny, L. Sannen, J. Nucl. Mater. 327 (2004) 121.
[9] C.R. Clark, S.L. Hayes, M.K. Meyer, G.L. Hofman, J.L. Snelgrove, Eighth International Topical Meeting on Research Reactor Fuel Management, Munich, Germany, March, 2004.
[10] G.L. Hofman, Y.S. Kim, H.J. Ryu, M.R. Finlay, Eleventh International Topical Meeting on Research Reactor Fuel Management, Lyon, France, March 11–15, 2007.
[11] K.H. Kim, D.B. Lee, C.K. Kim, G.L. Hofman, K.W. Paik, J. Nucl. Mater. 245 (1997) 179.
[12] T.C. Wiencek, Argonne National Laboratory Report No. ANL/RERTR/TM-15, 1995.
[13] S.L. Hayes, M.K. Meyer, G.L. Hofman, J.L. Snelgrove, R.A. Brazener, in: Proc. of the 23rd International Meeting on Reduced Enrichment for Research and Test Reactors, Chicago, Illinois, 2003.
[14] Y.S. Kim, Argonne National Laboratory, 2008, unpublished data.
[15] Y.S. Kim, H.J. Ryu, G.L. Hofman, S.L. Hayes, M.R. Finlay, D.M. Wachs, G.S. Chang, in: Proc. of the 26th International Meeting on Reduced Enrichment for Research and Test Reactors, Prague, Czech Republic, 2006.
[16] G.S. Chang, Idaho National Laboratory, 2008, unpublished data.
[17] D.E. Janney, A.B. Robinson, T.P. O'Holleran, R.P. Lind, M. Babcock, L.C. Brower, J. Jacobs, P.K. Hoggan, Hot Laboratories and Remote Handling Plenary Meeting, Bucharest, Romania, September 20–21, 2007.
[18] D. Olander, J. Nucl. Mater. 372 (2008) 94.
[19] F. Huet, V. Marelle, J. Noirot, P. Sacristan, P. Lemoine, in: Proc. of the 23rd International Meeting on Reduced Enrichment for Research and Test Reactors, Chicago, Illinois, 2003.
[20] S. Dubois, J. Noirot, J.M. Gatt, M. Ripert, P. Lemoine, P. Boulcourt, Eleventh International Topical Meeting on Research Reactor Fuel Management, Lyon, France, 2007.
[21] F. Huet, J. Noirot, V. Marelle, S. Dubois, P. Boulcourt, P. Sacristan, S. Naury, P. Lemoine, Ninth International Topical Meeting on Research Reactor Fuel Management, Budapest, Hungary, 2005.
[22] A. Leenaers, S. Van Den Berghe, E. Koonen, L. Sannen, M. Verwerft, C. Jarousse, F. Huet, M. Trotabas, M. Boyard, S. Guillot, Eighth International Topical Meeting on Research Reactor Fuel Management, Munich, Germany, 2004.
[23] A. Leenaers, S. Van Den Berghe, S. Dubois, J. Noirot, M. Ripert, P. Lemoine, Twelfth International Topical Meeting on Research Reactor Fuel Management, Hamburg, Germany, 2008.
[24] M. Ripert, S. Dubois, J. Noirot, P. Boulcourt, P. Lemoine, S. Van Den Berghe, A. Leenaers, A. Rohrmoser, W. Petry, C. Jarousse, Twelfth International Topical Meeting on Research Reactor Fuel Management, Hamburg, Germany, 2008.
[25] A. Leenaers, S. Van Den Berghe, M.C. Anselmet, J. Noirot, P. Lemoine, A. Rohrmoser, W. Petry, in: Proc. of the 28th International Meeting on Reduced Enrichment for Research and Test Reactors, Washington, DC, USA, 2008.

[26] J.M. Park, H.J. Ryu, Y.S. Lee, D.B. Lee, S.J. Oh, B.O. Yoo, Y.H. Jung, D.S. Sohn, C.K. Kim, in: Proc. of the 24th International Meeting on Reduced Enrichment for Research and Test Reactors, Vienna, Austria, 2004.
[27] J.M. Park, H.J. Ryu, Y.S. Lee, B.O. Yoo, Y.H. Jung, C.K. Kim, Twelfth International Topical Meeting on Research Reactor Fuel Management, Hamburg, Germany, 2008.
[28] J.M. Park, H.J. Ryu, S.J. Oh, D.B. Lee, C.K. Kim, Y.S. Kim, G.L. Hofman, J. Nucl. Mater. 374 (2008) 422.
[29] G.L. Hofman, L.C. Walters, in: R.W. Cahn, P. Haasen, E.J. Kramer (Eds.), Materials Science and Technology: A Comprehensive Treatment, vol. 10, VCH Publishers Inc., New York, 1994, p. 13.
[30] F. Mazaudier, C. Proye, F. Hodaj, J. Nucl. Mater. 377 (2008) 476.
[31] M.K. Meyer, G.L. Hofman, S.L. Hayes, C.R. Clark, T.C. Weincek, J.L. Snelgrove, R.V. Strain, K.H. Kim, J. Nucl. Mater. 304 (2002) 221.
[32] C.K. Varela, M. Mirandou, S. Arico, S. Balart, L. Gribaudo, Eleventh International Topical Meeting on Research Reactor Fuel Management, Lyon, France, 2007.
[33] S. Van den Berghe, W. Van Renterghem, A. Leenaers, J. Nucl. Mater. 375 (2008) 340.
[34] J. Rest, G.L. Hofman, Y.S. Kim, J. Nucl. Mater. 385 (2009) 563.
[35] K.-H. Kim, J.-M. Park, C.-K. Kim, G.L. Hofman, M.K. Meyer, Nucl. Eng. Des. 211 (2002) 229.